ELSEVIER

From biomaterial-based data storage to bio-inspired artificial synapse

Ziyu Lv [1,2], Ye Zhou [1,*], Su-Ting Han [1,*], V.A.L. Roy [3,*]

[1] College of Electronic Science & Technology and Institute for Advanced Study, Shenzhen University, Shenzhen 518060, PR China
[2] Key Laboratory of Optoelectronic Devices and Systems of Ministry of Education and Guangdong Province, College of Optoelectronic Engineering, Shenzhen University, Shenzhen 518060, PR China
[3] Department of Materials Science and Engineering, City University of Hong Kong, Hong Kong Special Administrative Region

The implementation of biocompatible and biodegradable information storage would be a significant step toward next-generation green electronics. On the other hand, benefiting from high density, multifunction, low power consumption and multilevel data storage, artificial synapses exhibit attractive future for built-in nonvolatile memories and reconstructed logic operations. Here, we provide a comprehensive and critical review on the developments of bio-memories with a view to inspire more intriguing ideas on this area that may finally open up a new chapter in next-generation consumer electronics. We will discuss that biomolecule-based memory employed evolutionary natural biomaterials as data storage node and artificial synapse emulated biological synapse function, which is expected to conquer the bottleneck of the traditional von Neumann architecture. Finally, challenges and opportunities in the aforementioned bio-memory area are presented.

Introduction

Noteworthy improvements in the performance of mobile phones, personal computers, TVs and other consumer electronics induce the explosive growth of requirement of information storage since memory is the main function of a computer in the contemporary era [1–17]. IC Insights predicted that total memory IC market will have 10% increment to achieve $85.3 billion which is mainly boosted by NAND flash and dynamic random access memory (DRAM) [18]. Nevertheless, large amounts of electronic wastes (e-wastes) are produced, and subsequently, an ecological problem occurs due to the short lifetime of silicon-based consumer electronics [19–21]. According to a report announced by the United Nations Environment Program, there are over 50 million tons of e-waste being generated and abandoned annually [22]. Besides, the recyclings of conventional e-wastes encounter enormous obstacles and challenges due to their diverse device structures and multi-functions. Furthermore, these e-wastes usually contain various non-degradable and toxic components with versatile properties, which not only affect the living environment but also are harmful to the human health [23]. Therefore, the implementation of biocompatible and biodegradable information storage would be a significant advance toward next-generation green electronics [24–29]. In another aspect, it is desirable to explore novel materials that are compatible with transparent, wearable, flexible, and minimization technologies because the continuous advances in silicon-based electronic devices are predicted to approach their fundamental physical limitations.

Natural biomaterials attract growing interests for the construction of implantable chips [30], electronic skin [31,32], biomedical diagnosis and therapy [33], artificial synapses, and neurons [34,35] since as-fabricated electronic devices are typically sustainable, biodegradable, biocompatible, and metabolizable. Besides above-mentioned advantages, biomaterials are lightweight, compatible with flexible substrate, cheap, and widely available. The exploration of electron transport progresses within biomaterials is the most crucial process for biological energy conversion, which can be realized in solid-state devices. Demands of future

* Corresponding authors.
E-mail addresses: Zhou, Y. (yezhou@szu.edu.cn), Han, S.-T. (sutinghan@szu.edu.cn), Roy, V.A.L. (val.roy@cityu.edu.hk).

https://doi.org/10.1016/j.mattod.2017.12.001

green data storage and novel electronics trigger advances in natural biomolecule-based memories. Furthermore, the biocompatibility and biodegradability of such biomolecule-based memory devices broaden their applications in implantable devices, biomedicine, and biosensing [36–39]. Some biomolecules including protein, sugar, DNA, RNA, and virus have been demonstrated to exhibit resistive switching behavior that is inherently robust-state transition, allowing the safe and "green" features into next-generation memory devices [40–52]. For example, bioresorbable silk produced by insects and spiders is a natural protein fiber mainly composed of fibroin [53–56]. Properties of lightweight, mechanical robustness, and optical transparency allowed the realization of a bio-compatible silk-based memory device with pronounced memristive switching effect [57].

On the other hand, conventional complementary metal-oxidesemiconductor (CMOS)-based volatile computers require frequent communications with external nonvolatile memories. The fundamental von Neumann architecture is nonscalable and inefficient to represent interconnected neural networks, inducing the von Neumann bottleneck and a gap between nonvolatile memories and microprocessors. In this respect, brain, central processing units of the human being, is the most sophisticated studying and simulating object given by nature. It can massively process various parallel information, while it consumes a very small amount of energy (1–100 fJ) per synaptic event [58–61]. Investigation reveals that the memory and study functions of brain originate from neuronal networks connected by numerous synapses (the amount is around 10^{15}) [62–68]. These synapses are functional links between nervous systems with a large amount of complex and random information flows inside [69–71]. Benefiting from high density, multifunction, low power-consumption, and multilevel data storage, artificial synapses exhibit attractive future for built-in nonvolatile memories and reconstructed logic operation, which is expected to bridge the above-mentioned gap. Thus, studying biological synapse, and then preparing artificial synapses to mimic the structure, as well as functions of biological synapse, provide a challenging and promising direction for the design and preparation of state-of-the-art memory. In recent years, different kinds of devices including filament-forming memristors [72–74], phase change memristors [75], and field effect transistors (FETs) [76–78] have been utilized to construct a series of artificial synapses. Synaptic functions such as spike-timing-dependent plasticity (STDP), long-term potentiation (LTP), long-term depression (LTD), paired-pulse facilitation, and self-learning ability have been mimicked through these synaptic systems [34,35]. Moreover, sophisticated and complex integrated neuromorphic networks have also been reported [79–83]. The study of artificial synaptic memory devices not only enable a better understanding of the principle of information processing in human brain [84] but also inspire novel design of bionic memory devices to improve the performance of computers [85].

Herein, we put forward a comprehensive and critical review on the developments of bio-memories with a view to inspire more intriguing ideas that may finally open up a new chapter in next-generation consumer electronics. This review paper is loosely grouped into two sections—biomolecule-based memory employing evolutionary natural biomaterials as data storage node and artificial synapse emulating biological synapse function that are expected to conquer the bottleneck of the traditional von Neumann architecture (Figure 1). In the first section, recent research progresses of biomolecule-based memory categorized by the biomolecules species, including protein, saccharide, RNA, DNA, and virus, are summarized. Advances in artificial synaptic memory constructed on filament-forming memristors, phase change memristors, and field effect transistors are then discussed in the second section. Last, challenges and opportunities in the aforementioned bio-memory area are presented in the conclusion section. This is a timely review that not only summarizes the recent advancements on the biomaterial-based memories but also proposes the prospective trend of artificial synapse that is of great importance to present many technological and academic opportunities in bioelectronics.

Biomaterial-based data storage

Natural materials possess nearly perfect structures and functions after millions of years' evolution in which the electron transfer is one of the most basic and elaborated biological processes [91]. Proteins are composed of at least one polypeptide chain with a specific 3D structure. Particularly, some redox proteins such as ferritin, myoglobin, and lysozyme, which normally contain multiple charge-trapping sites in their 3D structures, play key roles in a series of bio-electrochemical processes, including oxygen transport and storage, iron storage, and antisepsis. Reversible resistive switching of these proteins stemmed from redox reactions promises them as good candidates for RRAM devices and FET memories [92–94]. Natural polysaccharides are linear or branched biomolecules, which comprise long chains of D-monosaccharide units. Solid biopolymer electrolytes such as chitin and chitosan can be utilized as a thin active layer for data storage devices due to the utterly strong electron-trapping capacity and excellent processability of their primary amine and secondary amine groups [95,96]. In addition, DNA, which stores the genetic information of all natural creatures, processes the sophisticated double-helical structure with a π-stack core. The explorations of π-stack electron transfer have been widely performed by employing base pairs of DNA molecules as a versatile medium [97]. Besides, tremendous artificial DNA nanostructures with defined sequences of base pairs can be prepared through physical and chemical methods according to the Watson–Crick base pairing and the DNA assembly rules, suggesting its great potential for the application of nano electronic devices and photonic materials [98].

Here, representative works over the past decade of RRAM devices and flash memories constructed by various biomolecules, including protein, sugar, RNA, DNA, virus, and other natural biomaterials are summarized in this section (Table 1).

Protein-based memory

Proteins are the most common and easily accessible biomolecules in nature [99–101]. Reversible redox behavior (i.e., ferritin protein), electrical insulating properties, and resistive switching (RS) effect (i.e., silk protein) of proteins and peptides ensure them as promising building blocks for memory devices [24]. In 2010, Porath et al. demonstrated a nanoscale logic machine based on

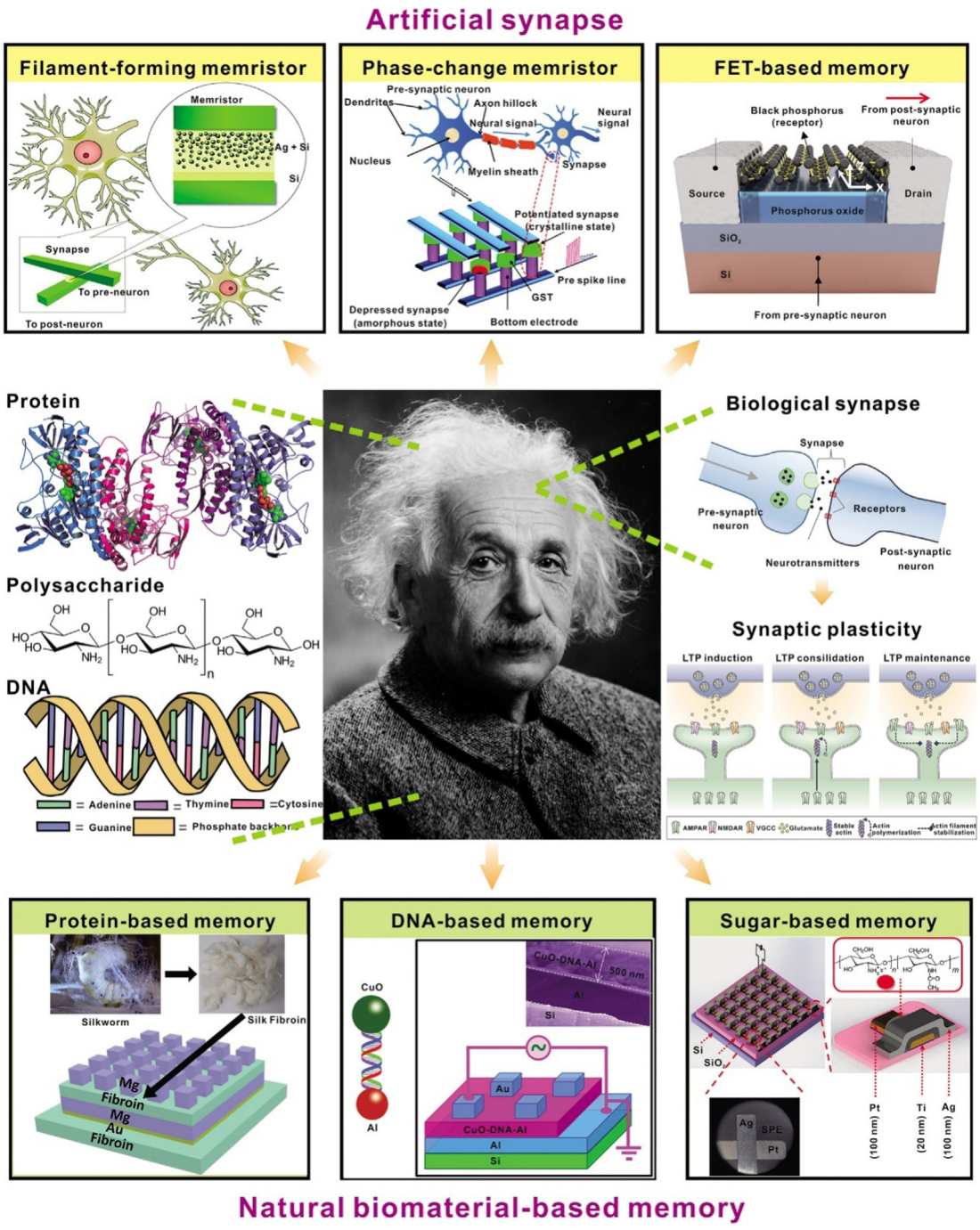

FIGURE 1

This review paper is loosely grouped into two section—biomolecule-based memory that employs evolutionary natural biomaterials as data storage node (below) and artificial synapse that emulates biological synapse function (top). A series of biomolecules (left) are used as versatile and sophisticated building blocks to construct memory devices exhibiting good biocompatibility and biodegradability; second, inspired by the most powerful biological memory system – brain (right), a numerous of artificial synaptic memory devices have been fabricated. Reproduced with permission [73,86–90].

a protein–nanoparticle hybrid consisting of a 5-nm silicon nanoparticle core and an SP1 protein shell [102]. SP1 protein constructed by 12 monomer units has a stable circular structure with an inner cavity. The good electrical isolation of the insulating SP1 provided finite capacitance of the nanoparticle core, thus endowing good stability of the logic machine. By virtue of a conductive atomic force microscopy (CAFM), cyclable set and reset operation and balanced temary logic implementation, as well as two-digit temary logic multiplication, were simultaneously implemented and observed in this nanoscale machine at room temperature.

Ferritin, a globular protein as a highly stable iron-storage container, can release and store iron in a controlled manner. In response to an external electric field, the shell of ferritin can release iron ions and then induce distinct RS effect. In 2011, Cho et al. utilized ferritin nanoparticle multilayers as functional

TABLE 1

Data storage devices based on various natural biomolecules, including protein, saccharide, DNA, RNA, and virus.

Biomolecules	Device terminology	Device type	Structure	ON/OFF ratio	Cycle number	Retention time	Refs
Protein	Ferritin	RRAM	Pt/PAH-Ferritin Multilayer/Ag	10^6	300	10^4	[103]
	Silk fibroin	RRAM	Ag/silk fibroin/Au	10^5	30	10^4	[106]
Saccharide	Chitosan	RRAM	Ag/Ag-doped chitosan/Pt	10^5	100	10^4	[87]
	Maltoheptaose	Flash memory	Au/pentacene/maltoheptaose/SiO_2/Si	10^6	/	3.6×10^4	[107]
DNA	CuO-DNA-Al	RRAM	Au/CuO-DNA-Al/Au/Si	50	100	10^3	[88]
RNA	RNA	Molecular memory	QD-STV/RNA/Au	100	/	10^6	[109]
Virus	Tobacco mosaic virus (TMV)	RRAM	Al/TMV-Pt nanoparticles/Al	10^3	400	10^4	[111]

layers to construct nonvolatile RRAM device [103]. The memory properties of ferritin films investigated by theKelvin force microscopy indicated that the core of this ferritin protein could reversibly trap and release Fe^{3+}/Fe^{2+} in response to an external voltage, which endowed the protein films with switchable resistance. In addition, with the increase in the thickness of anionic ferritin nanoparticles (NP) and cationic poly-(allylamine hydrochloride) bilayer, the OFF current decreases dramatically since the external electric field level is lowered by the multilayer with increased thickness. Subsequently, the remarkable improvement of the device's ON/OFF current ratio was obtained. In 2013, the authors further incorporated discrete ferritin nanoparticle with pentacene to fabricate field-effect transistor (FET) flash memories (Figure 2) [94]. The devices exhibited nonvolatile memory properties with reversible threshold voltage shifts originated from charge trapping and detrapping of the ferritin NP-based gate dielectrics. A large memory window of 20 V, a high ON/OFF current ratio of 10^4, and a fast switching speed of 10 μs could be achieved in ferritin NP-based FET memory devices. Moreover, flexible protein-based flash memories were fabricated on plastic poly (ethylene naphthalate) substrates pre-deposited with Al_2O_3 gate dielectric layer. In 2012, the authors reported a FET-based flash memory device using another redox protein–myoglobin as a charge-trapping layer [92]. Myoglobin, containing a heme structure and mainly existing in muscle tissue, plays a key role in oxygen transport. The transfer characteristics of the FET memory devices exhibited a nonvolatile memory effect which may be stemmed from the reversible redox reactions of Fe^{2+}/Fe^{3+} in the heme structure. In 2016, Hao et al. reported a ferritin-based RRAM with novel RS characteristics, in which nonvolatile memory mode and volatile memory mode can be alternatively switched between each other via readily adjusting the magnitude of compliance current (CC, 100 nA for nonvolatile mode and 100 μA for volatile mode) [93]. In 2011, Chen et al. demonstrated ferritin-based bipolar memristive nanodevices that consisted of On-wire lithography (OWL) nanowires with a ferritin-modified nanogap (diameter: 12 nm) [45]. The high electrochemical activity of the protein core endowed ferritin with a

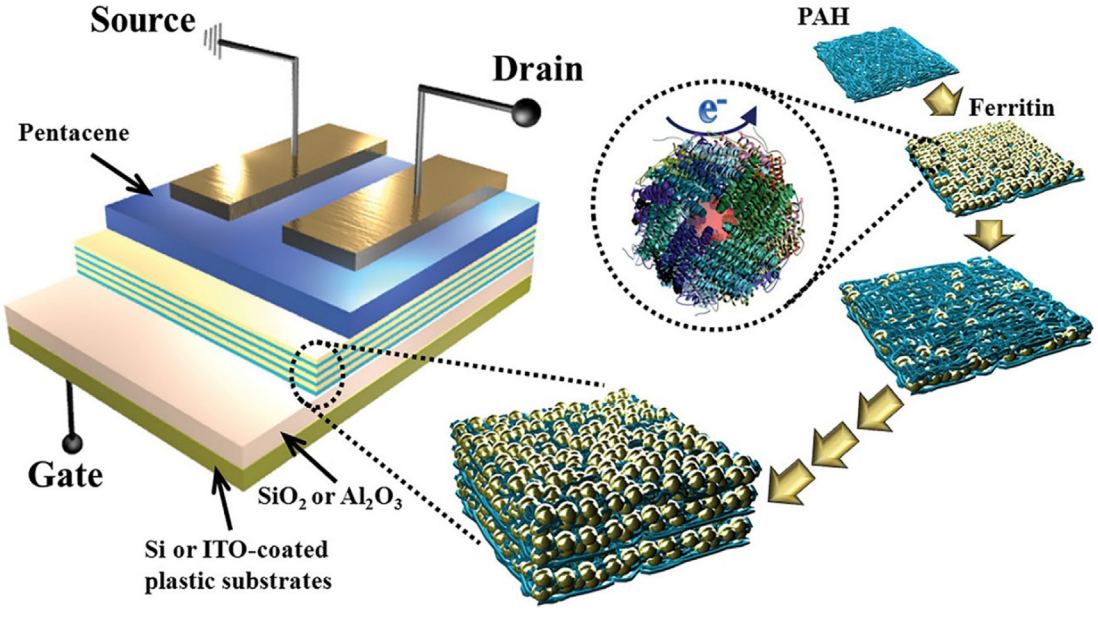

FIGURE 2

Schematic illustration of the FET memory device using Layer-by-Layer-assembled (poly(allylamine hydrochloride)/ferritin NP)$_n$ multilayers as gate dielectrics. Reproduced with permission [94].

large ion-loading capacity, thereby improving the memristive performance of the nanodevices. Nonvolatile memory behavior of these protein-based nanodevices was also demonstrated in write-read-erase cycle tests. Moreover, ferritin with a unique cage structure (7-nm inner diameter and 12-nm outer diameter) was also employed to assist homogeneous dispersion of Pt nanoparticles (Pt NPs) in an RRAM device. In a slow reaction system, ferritin crystallized Pt NPs inside its spherical cavity by biomineralization. The excellent dispersion of Pt NPs in insulating layer enabled a controllable forming of the conductive filament, thereby improving RS effect in the device.

Silk fibroin is another representative biomolecule that is highly recommended as building blocks of RRAM devices due to its advantages including mechanically superior, optical transparency, and capable of processing in aqueous environment [24]. Bera et al. reported bio-RRAM devices based on pure silk fibroin protein [104]. The oxidation state and reduction state of the silk fibroin film could be obtained through the treatment of positive and negative bias, respectively. These two states of the silk fibroin film according to low and high resistances allowed the protein film with resistive switching ability.

Chen's group in Nanyang Technological University published a series of works on the demonstration of silk fibroin-based RRAMs. In general, the RS effect of memories can be categorized according to volatility, namely memory RS (nonvolatile) and threshold RS (volatile). Although a number of protein-based memory devices display RS effect, it is still a challenge to fabricate memory devices with tunable RS effect. Interestingly, in 2015, Chen's group reported a silk protein-based memory with tunable RS modes between memory RS mode and threshold RS mode through regulating the CC in the set process (Figure 3) [105]. The memory RS and threshold RS were obtained by the application of a high CC (>100 μA) and a low CC (<10 μA), respectively (as shown in Figure 3a and b). Mechanism studies revealed that the formation of electron-conductive pathways of Ag nanoparticles in the silk layer determined the RS mode of the protein-based devices. Furthermore, both random access mode (reversible switching) and write-once-read-many-times (WORM) mode grounded on this RS effect, exhibited extremely high OFF/ON ratio of 10^8 and long retention time of 10^4 s. In 2016, the same group further fabricated RRAMs based on silk protein with an architecture of Au/Mg/fibroin/Mg [86]. The devices can be gradually decomposed in water or PBS solution within 2 h at room temperature due to water solubility of silk fibroin layer and active reaction between water and Mg electrodes. This transient behavior may open up a new prospect for the development of implantable chips and biodegradable memory devices. Recently, the authors advanced their research by constructing ultra-lightweight RS silk-based memory devices [106]. By utilizing a silk substrate and well-designed fabrication memory procedures, the weight of the RRAM device is reduced to 0.4 $mg \cdot cm^{-2}$, which is much lighter than that of the device fabricated on conventional silicon substrate or office paper. By adding NPs into silk fibroin matrix, the performance of the protein-based memories can be further improved. In 2013, Gogurla et al. reported a flexible RRAM device ground on the silk fibroin matrix embedded with Au NPs [44]. A higher ON/OFF ratio and a lower set/reset voltage were realized in this device. The authors assumed that the formation of electron-conductive paths in the protein layer induced by the Au NPs/silk nanocomposite was the main operation mechanism of the memory device.

Saccharide-based memory

Besides proteins, saccharides, especially polysaccharides, are being widely used as building blocks for the development of novel green memory devices. Saccharide contains large amounts of hydroxyl groups, of which the dipole orientation can be modulated by the application of external voltage. Hence, saccharide can serve as an electron-accepting layer in flash memory devices to ensure hysteresis effect. In 2015, Chen et al. reported pentacene-based transistor memory devices by utilizing oligosaccharide maltoheptaose (MH, a linear α-1, 4-glucan) as the dielectric layer [107]. Two distinct current states were obtained after application of programming/erasing operations of ±50 V gate-source pulses for 2 s, respectively. These flash memories exhibited a positively shifted transfer characteristics after both programming and erasing processes, indicating that a unipolar electron-trapping property of the MH layer. It should be noted that the high-conducting state was settled down in the MH layer as a result of deep electron-trapping behavior after consecutive application of two positive biases.

Chitosan, a ubiquitous polysaccharide comprised of stochastic arranged N-acetyl-D-glucosamine and β-(1-4)-linked D-glucosamine, has attracted increasing research interest in the development of RRAM devices. Lee et al. systematically studied a series of flexible bio-RRAMs by employing the natural solid polymer as a resistive switching layer. In 2015, they utilized Ag-doped chitosan as RS layer to fabricate redox-based RRAMs [87]. The chitosan layer could be controlled reversibly between high- and low-conducting states through alternatively applying positive and negative biases. The bipolar resistive switching characteristics of the memory devices were proposed to be originated from formation and rupture of the filament. Subsequently, a transparent RS employing a cell architecture of Mg/Ag-doped chitosan/Mg on transparent and bendable polyethylene terephthalate substrate was further demonstrated (Figure 4) [95]. The device displayed a long data retention time, a reasonable ON/OFF current ratio, as well as low-power operation with superior mechanical property. As shown in Figure 4c–f, good water solubility of each component of the chitosan-based devices promised complete decomposition of the devices within approximately 10 min via the treatment of DI water. In 2016, the authors advanced their investigation by integrating chitosan with potato starch as an active layer to fabricate RRAM device [96].

RNA- and DNA-based memory

Accompanied with the development of RNA and DNA nanotechnology, both RNA and DNA can serve as a versatile and powerful material to enable the construction of numerous novel nanostructures and nanodevices through a predictable base-pairing rule [49,98,108]. In 2015, Guo et al. reported a resistive biomemory system based on an RNA-QD (quantum dot) chimera in which the pRNA-3WJ motif acted as the feet on the Au substrate and a streptavidin-coated QD served as the head [109]. The RNA-based insulated layer could act as a mediator to ensure the fixed distance between the QD head and the Au substrate. This

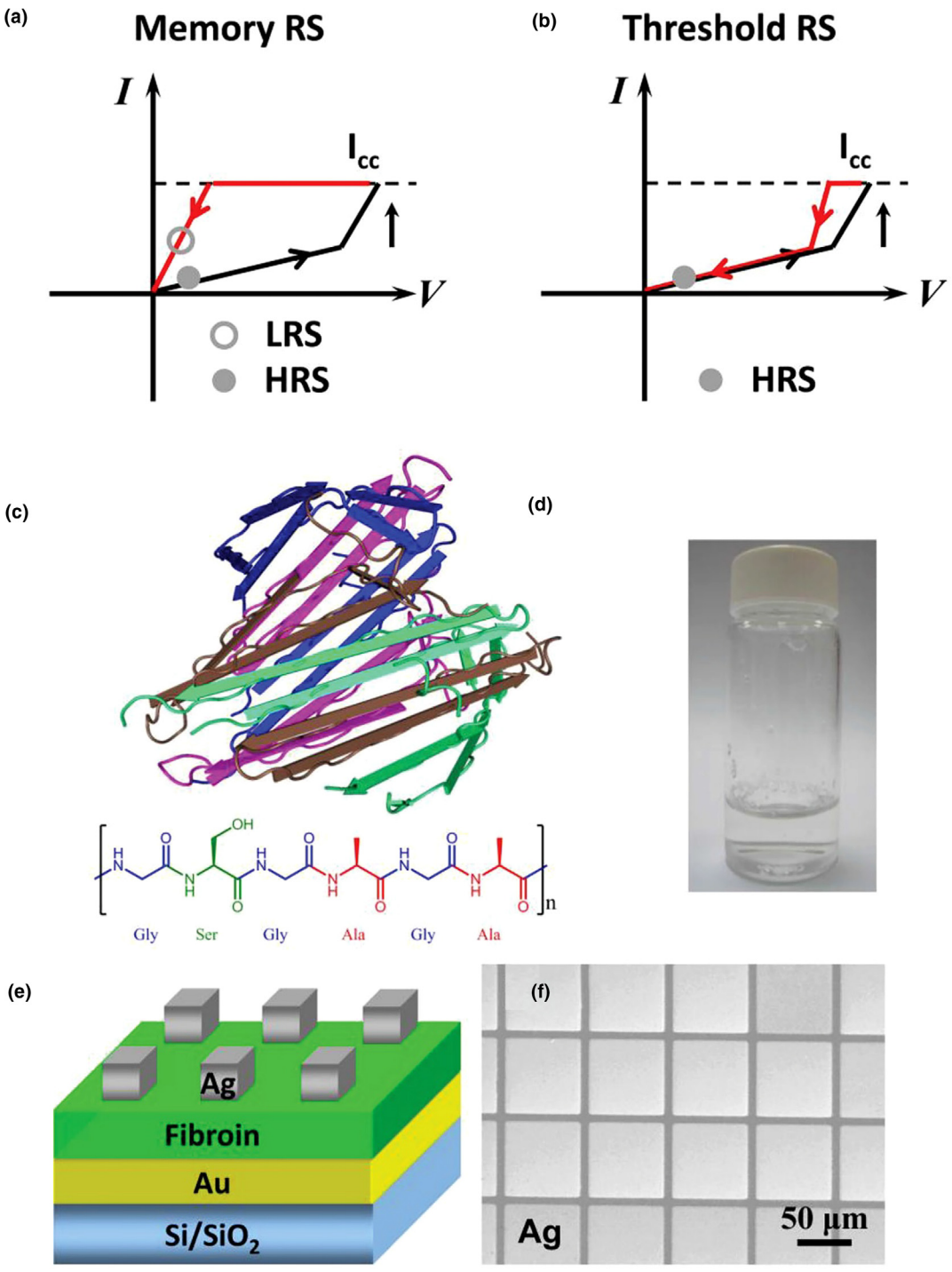

FIGURE 3

Schematic illustrations of I–V characteristics of silk-based memory RS effect (a) and threshold RS effect (b). Without applying an external voltage, memory RS experience reversible alternation between low and high conductive state. In contrast, threshold RS only exhibit high resistance state. (c) Secondary structure (top) and primary structure (bottom) of silk fibroin. (d) Optical image of silk fibroin aqueous solution. (e) Schematic illustrations of the device structure with an active silk fibroin layer. (f) Scanning electronic microscopy (SEM) image of the device arrays. Scale bar: 50 μm. Reproduced with permission [105].

RNA-inorganic chimera nano-system exhibited great potential as nano-bioinspired memory systems due to its distinct resistive switching effect. In 2015, Chen et al. fabricated DNA-based RRAM through DNA-directed assembly procedure in which a double-stranded DNA served as a bridge to connect CuO and Al nanoparticles [88]. In contrast to CuO-Al nanocomposites, the CuO-DNA-Al nanocomposites displayed considerably improved bipolar resistive switching memory characteristic. The mechanism study suggested that the DNA linker could stimulate the formation and inhalation of conductive filament between Cu and Al nanoparticles, thus improving resistive switching effect of the CuO-DNA-Al nanocomposites. In 2015,

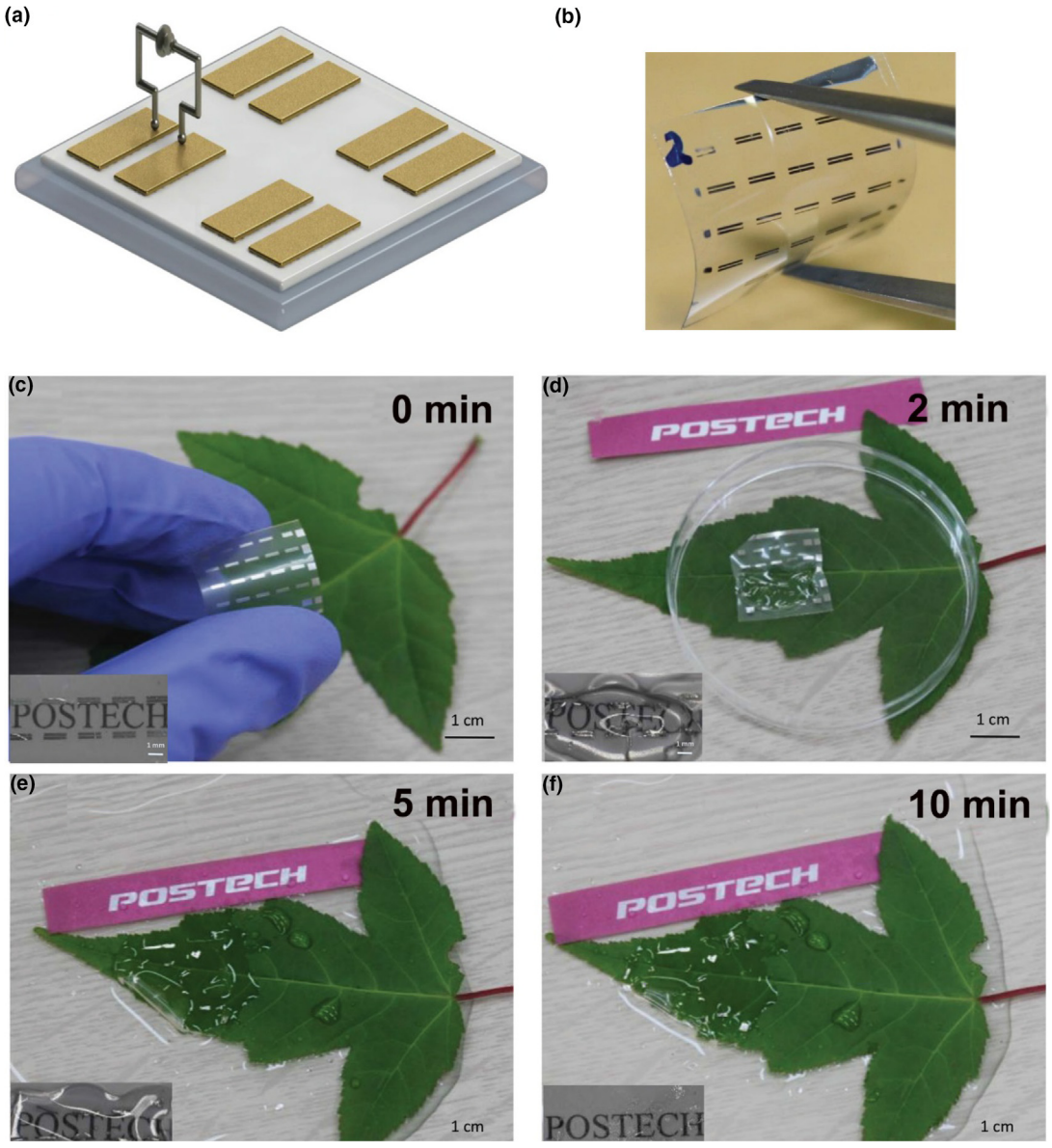

FIGURE 4

Schematic illustration of (a) memory device with an active Ag-doped chitosan layer and (b) image of the flexible and transparent memory devices. The decomposition process of biodegradable and transparent memory devices with a paper-chitosan substrate, triggered by the treatment of DI water: (c) 0 min, (d) 2 min, (e) 5 min, and (d) 10 min. Scale bar: 1 cm. Reproduced with permission [95].

Dong et al. reported a multilevel bio-RRAM composed of multilayer pure DNA molecules and Au electrode [49]. Excellent properties such as long retention time, good sweep endurance, and reproducible WORM behavior were observed. In addition, multilevel memory behaviors could be realized in this biomemristor via application of various sweeping voltages. In 2007, Singh et al. also reported a FET memory using (hexadecyltrimethyl ammonium chloride) CTMA-modified DNA as gate dielectric [110]. Transfer characteristics of this DNA-based FET demonstrated a nonvolatile memory behavior and a significant hysteresis effect in a low operating voltage. Besides, hysteresis effect could be regulated by embedding a thin blocking (Al_2O_3) layer between the CTMA-modified DNA layer and the semiconductor layer.

Virus-based and other biomolecule-based memory

Memory devices can be constructed by many biomolecules, such as peptide, protein, saccharide, and DNA. Besides these above-mentioned biomaterials, tobacco mosaic virus (TMV) can be used as basic building blocks to fabricate memory device as well. TMV is composed of approximately 2130 molecules of identical coat protein units, and a single RNA molecule which exhibits a tube-shaped structure with a 4-nm-wide inner diameter and an 18-nm-wide outer diameter. TMV has been utilized in the potential applications, including electronics, energy storage, and drug delivery. In 2006, Yang et al. reported nonvolatile memory constructed on the hybrid of TMV and platinum nanoparticles (Pt NPs) in which TMV served as charge donors since its RNA segments are rich in aromatic rings (e.g., guanine)

[111]. The memory effect was derived from the conductance switching inside the bio-inorganic nanostructures that induced bistable states with a high current ON/OFF ratio more than 10^3. The mechanism study suggested that the application of high electric field could tempt charge transfer from the RNA core to the Pt NPs and further triggered a remarkable variation of the bio-hybrid conductivity.

Various kinds of novel natural materials have also been used as building blocks for developing data storage devices. In 2014, Wang et al. demonstrated a reproducible and bipolar RS effect via a gelatin-based RRAM system with a structure of Al/gelatin (35 nm) /ITO [46]. The energy-dispersive X-ray and current-sensing AFM investigations of the memory indicated that the reproducible RS effect was dictated by metal conductive filament formation. A similar data storage device based on eggshells was reported by Wu et al. [112]. Formation and destruction of Ag filament were proposed as the decisive factor for realizing the nonvolatile RS memory behavior. In 2017, Lee et al. utilized lignin as an active layer to prepare a multistate RRAM device on a flexible PET substrate [113]. The I–V characteristics of Au/lignin/ITO/PET cells indicated that four unique resistance states could be achieved through modulation of compliance current and reset voltage. Besides, an RS behavior of the device with no fluctuation after repetitively bending treatment certified the bending stability.

In this section, biomaterial-based data storages have been summarized. Biomolecules can be used as active layers to construct RRAM devices, dielectric layers to fabricate flash memories, or insulating cavity for built-in logic memory. In addition, large biomolecules such as silk and chitosan can be also employed as novel substrates for developing biocompatible, flexible, and lightweight memory devices.

Artificial synapses

Besides biomolecule-based data storage devices, another attractive research field is to study biological memory systems and then emulate both the structures and memory functions of these systems [89,114–118]. Specially, brains are the most powerful and exquisite memory systems, of which the storing and processing of massively parallel information can be achieved through adjusting the strength of the synaptic connection (synaptic weight), while theyoffer a sophisticated space and energy tradeoff. Typically, a chemical synapse, consisting of axon terminal, synaptic cleft, and dendrite, is regarded as a functionalized linker that permits neuron to transmit neurotransmitters to another adjacent neuron. Synaptic plasticity and memory (SPM) hypothesis suggests that a basic and decisive factor for achieving memory and learning ability is synaptic plasticity, which is identified as the capacity of synapse to strengthen or weaken on account of an alteration in its neuronal activity [119]. According to the length of lasting time, synaptic plasticity can be divided into short-term plasticity (short-term potentiation and short-term depression) and long-term plasticity (long-term potentiation and long-term depression). Particularly, long-term potentiation (LTP), one of the most studied forms of synaptic plasticity, takes a vital role in the consolidation of memory and formation of long-lasting memory as a result of a permanent alteration in synaptic connection strength [120]. Experiment with mutant mice also indicated that hippocampal LTP behavior and spatial learning depended on the same cellular mechanism [121]. Therefore, the preparation of artificial synapses and subsequent emulation of predominant activity-dependent synaptic plasticity such as LTP, long-term depression (LTD), short-term potentiation (STP), short-term depression (STD), and spike-timing-dependent plasticity (STDP) will provide great benefit in the development of highlyintegrated and low-power-consumption memory device [82,85]. For the development of artificial synapses and synaptic systems, materials should at least process two basic characteristics. First, biological synaptic systems can build a relationship between their responsiveness and input stimuli history. Thereby, materials should work as a multi-state memory and in response to the same repetitive external input stimuli since they are supposed to stay in a certain state depending on the input history. Second, in order to avoid refreshing or energy dissipation in the storage of the memory state, the nonvolatile characteristic of memory elements is indispensable. So far, classified by existing device architectures including filament-forming memristor, phase change memristor, and FET device, we summarized the recent artificial synapses in this research area.

Filament-forming memristive synapse

Memristors are basically two-terminal special RRAM devices, of which conductance is governed by the times of external applied voltage/current [122]. Particularly, conductive filament-forming memristors and memristive systems that are inherently dynamic memories with fast speed and low powerconsumption have been demonstrated with hopeful prospects for the development of nonvolatile data storage devices and computing applications. The conductance change of filament-forming memristor is ascribed to the formation and rupture of an electron-conducting path in an insulating layer, triggered by ion migration or redox reaction of the active electrode. Notably, resistive switching behavior of filamentary memristors is quite analogous to the change in synaptic weight refereeing to the strength of adjacent synaptic connection. Consequently, filament-forming memristive system has been regarded as a suitable candidate for efficiently emulating both synaptic structures and functions in biologically neuromorphic systems. So far, a number of filamentary memristors, particularly metal-oxide ones, have been employed as artificial synapses to emulate critical synaptic learning rules including LTP, STP, STDP, paired-pulse depression (PPD) and paired-pulse facilitation (PPF).

Biomaterial-based memories have recently been demonstrated to function as non-volatile data storage for emulation of synaptic functions including LTP, STP, STDP, PPD, and PPF. A large renewable biopolymer such as lignin can be utilized as an active layer in filament-forming memristive-architectured synapse. Lee et al. emulated synaptic behaviors such as STP, LTP, spike-rate-dependent plasticity, and short-term to long-term transition based on lignin-based RRAM system with a structure of Au/lignin/ITO/PET [123]. Implementation of synaptic behaviors did not exhibit significant flutation under bending test, suggesting its excellent stability. Formation and rupture of unstable filament under external electrical bias were assumed as the mechanism of these different synaptic functions.

Lu's group in University of Michigan has fabricated a number of memristor devices as synapses in neuromorphic systems. In 2010, Lu et al. demonstrated a crossbar-configurated neuromorphic system which is composed of complementary metal-oxide semiconductor (CMOS) neurons and memristor synapses [73]. Benefiting from the crossbar configuration, every presynaptic neuron has its own connection to a corresponding postsynaptic neuron with unique synaptic weights. Ag-rich region with low resistance and an Ag-deficient region with high resistance were generated from the gradient doping of Ag NPs in Ag/Si active layer. The resistance of the memristor was incrementally modulated through the controllable shift of Ag nanoparticles between Ag-rich region and Ag-deficient region triggered by the application of external voltage bias. Emulation of synapse functions such as spike-timing-dependent plasticity (STDP) was facilitated by this characteristic. The well-fitted memristor synaptic weight change versus the neuron spikes' timing difference further confirmed the STDP characteristics of the memristor synapses. Besides, the authors fabricated a series of tantalum oxide-based memristors with controllable resistive switching characteristics, fast switching speed, and excellent endurance property to demonstrate that this artificial memristor synapse is capable to realize more sophisticated synaptic functions [124,125]. Notably, Mimicking Ca^{2+}-like dynamics in memristor should be projected in pursuit of more complicated artificial synapse since Ca^{2+} dynamics including the accumulation and extrusion of Ca^{2+} play a vital role in synaptic plasticity. In 2015, the same group exploited a second-order drift memristor (i.e., tantalum oxide-based memory) as synapse to realistically implementation critical synaptic functions such as frequency-dependent plasticity and timing-based plasticity [126]. Particularly, instead of using complex overlapping spikes or programming waveform designed in first-order memristor, the authors utilized Ca^{2+}-like short-term temperature dynamics of the memristor to encode information on the relative spike timing and synaptic activity. In 2017, Yang and co-workers demonstrated Ag nanocluster-in-oxide-based memristors, in which the Ag atoms' diffusive dynamics was analogous to the Ca^{2+} migration in biological synapse (Figure 5c) [74]. The architecture of memristors was a SiO_xN_y dielectric layer doped with Ag nanocluster sandwiched between two inert electrodes (Pt or Au) (Figure 5a). The Ag-in-oxide memristors exhibited a quite large resistance ratio of 1×10^5 between low-conductance state and high-conductance state so that preformed sneak current paths in crossbar devices can be depressed. The bridge effect originated from Ag migration played an important role in the RS behavior, which was proved by *in situ* high-resolution transmission electron microscopy (HRTEM), as displayed in Figure 5b. Ag atoms dispersed under an external electric field and then aggregated into nanoparticle spontaneously under zero bias as a result of interfacial energy minimization. As shown in Figure 5d, natural emulations of short-term synaptic plasticity including PPF and PPD behavior, as well as PPD following PPF behavior, were achieved in the diffusive Ag-in-oxide memristors.

Constructing artificial synapses with both short-term plasticity (STP) and long-term plasticity (LTP) is particularly attractive since the mechanism of human memory is mainly attributed to these two types of synaptic plasticity. In 2011, Ohno and coworkers fabricated an Ag/Ag_2S/nanogap/Pt synapse in which a transition from synaptic functions STP to LTP was achieved by adjusting repetition time of input pulse, as shown in Figure 6a [62]. By applying input pulses, an Ag conductive pathway between the Pt electrode and the Ag_2S electrode was formed as a result of the migration of Ag atoms toward the top Pt electrode, which referred to LTP, while the state referred to STP when the bridge was destroyed. The triggered high conductance of the inorganic synapse decayed to initial low conductance with stimulus pulses with intervals of 20 s, which resembled STP behavior in biological synapses (Figure 6b). In contrast, the conductance of the synapse was maintained at a high level with stimulus pulses with intervals of 2 s. Subsequently, the authors advanced their study based on the similar Cu/Cu_2S/nanogap/Pt memory system [127]. In addition to adjustment of input pulse stimulation, the synaptic plasticity of the synaptic device could be modulated by temperature and humidity. In 2013, Palma and co-workers reported a stochastic neuron based on an Ag/GeS_2 conductive bridge memory system [128]. During the set process, a stochastic firing behavior could be implemented. Most recently, Park and co-workers prepared a $Ag/PbZr_{0.52}Ti_{0.48}O_3$(PZT)/$La_{0.8}Sr_{0.2}MnO_3$(LSMO) conductive bridge memory-based synapse [129]. Instead of applying an external electric field, the ultrathin PZT layer (4 nm) could act as a selective electrolyte to trigger ion migration and diffusion, selectively activating the synaptic plasticity, as well as the transition from STP to LTP. The synaptic device exhibited low energy consumption, ultrasmall dimensions, and fast speed of programming.

Besides synaptic emulators, several groups utilized metal-oxide memristors to act as synaptic units for fabrication of more complicated integrated neuromorphic networks. In 2015, Prezioso and co-workers demonstrated an operational neuromorphic network via a highly integrated transistor-free metal-oxide (Al_2O_3/TiO_{2-x}) memristor crossbar [80]. The memristor crossbar exhibited low variability, low switching and forming voltages (with 2 V), low operation currents, high ON/OFF current ratios, and good endurance properties. Benefiting from these characteristics, a crossbar network, containing ten input elements and three elements, could completely *in situ*divide the pattern classification of 3×3 -pixel black-and-white images into three categories by utilizing a delta rule algorithm. This study points out a clear direction for designing mimetic synapses with smart features to perform complex and sophisticated tasks. In 2015, Hosaka et al. demonstrated an associative memory possessing the ability to retrieve the whole block of data from a segment of data based on a HfO_2-based memristive Hopfield network [130]. The synaptic weights of the memristive network could be well modulated through adjusting the resistance of the HfO_2-based memristors, enabling the storage of different pattern information into the memristive Hopfield network. In 2016, Serb et al. reported TiO_2-based memristive synapses with gradual, intrinsic, and multilevel resistive switching characteristics [79]. The encoding and storage of conditional probabilities in different conductive states of these multistate memristors were achieved. Moreover, the emulations of biological weight-dependent plasticity, including reversible learning and unsupervised learning, as well as forgetting, were demonstrated in probabilistic neural networks through these memristive synapses.

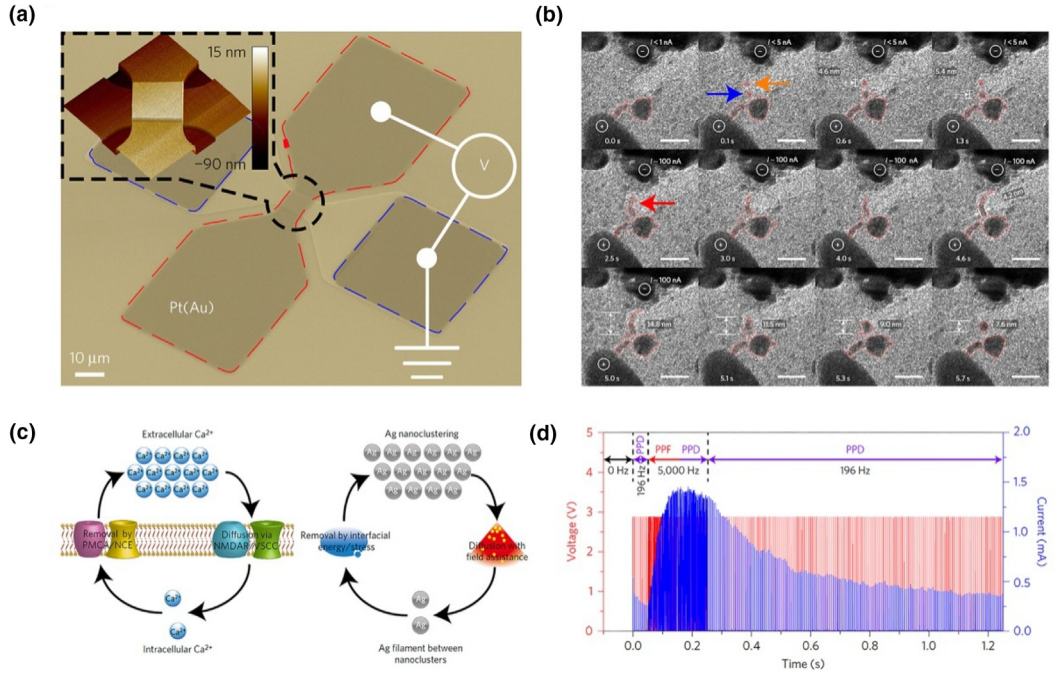

FIGURE 5

(a) Pseudo-color SEM image of a micro-memristor that composed of two inert electrodes (i.e., Pt or Au) sandwiching a SiO_xN_y dielectric layer embedded with Ag nanocluster. (b) The study of the threshold switching behavior via *in situ* HRTEM observation. These HRTEM images indicate that the driven force of the diffusive dynamics is an interfacial energy minimization. (c) Schematic illustrations of the similarity between biological synaptic Ca^{2+} dynamics and Ag atom dynamics of the diffusive memristor. (d) The simulation of synaptic PPF and PPD behavior, as well as PPD following PPF behavior by the Ag-in-oxide memristors. Blue line: the memristive device current; red line: applied voltage pulses with uniform amplitude (2.8 V) but different frequencies. Reproduced with permission [74].

Phase change memristive synapse

Phase change materials display reversible and rapidly switching behavior between an amorphous phase and a crystalline phase through applying a suitable current pulse (amplitude and duration) to generate enough heat for phase transformation [131]. As a result of different bonding mode, the amorphous phase and crystalline phase exhibit quite diverse structures in term of their structural periodicity and long-range order, which then induce distinct electrical and optical characteristics [131]. For application of these materials in phase change memory (PCM), amorphous state and crystalline state usually refer to low conductance state and high conductance state, respectively. PCM materials have already been utilized in practical applications such as rewritable optical storage devices (i.e. compact disks (CD) and digital versatile disks (DVD)) due to their impressive ON/OFF current ratio, long retention time, satisfactory endurance, and high yield characteristics. Stability of the amorphous state and the crystalline state under operating temperature is another merit of PCM materials. In addition, large-array PCM materials can be readily integrated in small device dimensions without compromising on device performance, suggesting its appropriateness for simulation of biological synapses and neural networks [132].

Chalcogenide glass, more specifically a ternary alloy $Ge_2Sb_2Te_5$ (GST), is one of the most extensively used materials for PCM applications [133]. In 2012, Kuzum and co-workers fabricated crossbar array-architectured nano-scale synapses based on GST phase change materials with ultrahigh density and excellent compactness (Figure 7a) [90]. Set and fully reset states, in which the resistance of GST layer reversibly varied from low resistivity of 500 Ω to high resistivity of 2 MΩ, were obtained through the application of electric pulse stimuli (Figure 7b). Benefiting from a fine modulation of intermediate resistance levels in PCM materials, different forms of STDP behaviors consuming just picojoule-level energy were achieved. It is worth noting that emulating different forms of STDP is of great importance since the form of STDP is regarded as the key step for plasticity modeling. In this GST-based system, four forms of STDP, including asymmetric STDP with potentiation/depression and symmetric STDP with potentiation/depression, were emulated, as shown in Figure 7d. In 2013, a similar GST-based synapse with a T-structure has been reported by Li et al. [134]. Through regulating the electrical pulses, the resistance of this GST-based device could be fine modulated. Due to the fast and reversible phase transition of GST layer, ultrafast STDP events of this PCM synapse could be successfully implemented through the treatment of pre-/post-synaptic spiking pulse pairs.

In biological synapse, the potential of a lipid-bilayer membrane can be maintained because the internal electrical charges of the cell are separated from the outside ones by the membrane. The action potentials induced by the excitatory or inhibitory postsynaptic potentials influence membrane potentials accordingly. Simulation of the equilibrium potential maintenance is another figure of merit for the fabrication of novel neuromorphic computing systems. In 2016, Tuma and co-workers reported a stochastic phase change device, in which biological stochastic

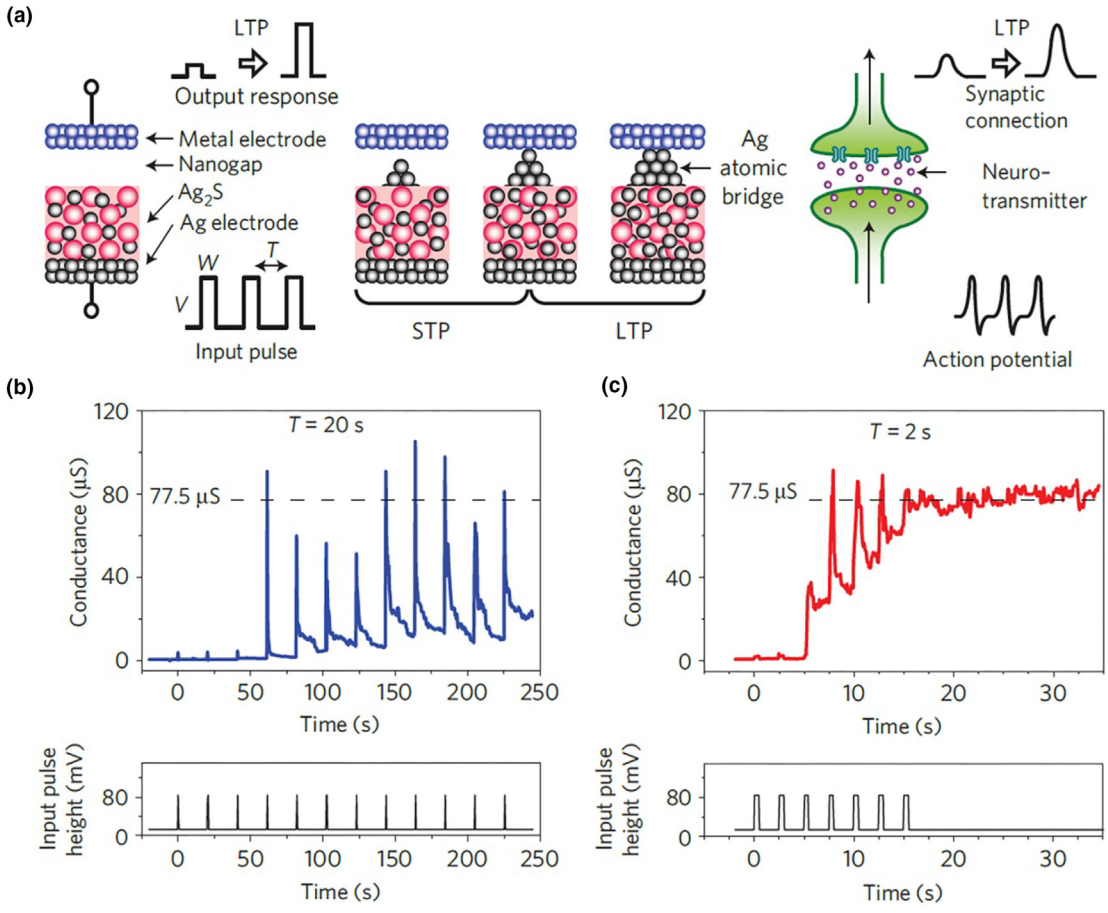

FIGURE 6

(a) Schematic illustration of the Pt/nanogap/Ag_2S/Ag inorganic synapse and its signal transmission. By applying input pulses, an Ag conductive pathway between the top Pt electrode and the Ag_2S electrode formed, as a result of the migration of Ag atoms toward the top Pt electrode. With stimulus pulses at intervals of 20 s (b) and 2 s (c), the decay behaviors of the triggered high conductance of the synapse, behaves as STP (b) and LTP (c), respective. Reproduced with permission [62].

dynamics of membrane potential were well emulated [75]. The mushroom-type phase change device was composed of a nanoscale volume of GST-based phase change materials (thickness: 100 nm) sandwiched between top and bottom electrode (Figure 8a). The initial state of GST materials of the as-fabricated device was crystalline with low resistivity. The conductance of this phase change neuron could be well controlled through manipulating the width and power of the set pulse, as well as the subsequent reset pulse (Figure 8b). Furthermore, the authors investigated the temporal correlations between neuronal input and conductance of a single phase change neuron. Initially, the vast majority of dense neuron-firing events were induced by uncorrelated presynaptic spikes (Figure 8c). The neuron fires were closely correlated to the presynaptic spike events after the convergence of neuronal input, thus giving rise to a progressive increase in the synaptic weights. Stochastic dynamics behavior was also emulated based on the inherent stochasticity of GST phase change materials. Distribution of interspike intervals was generated by multiple integrate-and-fire cycles in a phase change unit. As displayed in Figure 8d, the interspike intervals distributed normally with large pulse widths.

Besides GST-based materials, NbO_2 phase change materials have also been integrated into artificial synaptic devices [135]. Instead of the phase transformation between amorphous and crystalline state, NbO_2 phase change materials experience reversible phase transitions between metallic and insulating state when electric pulses cross over the materials and sufficient heat was generated for phase transition. A research group of HP labs has exploited NbO_2 phase change material for the development of a neuristor circuit system; neuron-like spiking behavior in the system was emulated as well [136].

Field effect transistor-based synapse

Besides filament-forming memristive synapses and phase change memristive synapses, there are also increasing efforts ongoing to prepare field effect transistor (FET)-based synapses [137]. Memristive synaptic devices are always suffering from disability of simultaneously accomplishing signal transmission and learning event because only a single path available between pre-synapse and post-synapse to deliver neural signals or regulate the synaptic weight to achieve learning functions. However, three-terminal FET-based synapses can figure out this limitation by the virtue of delivering signals via their channel mediums and modulating the synaptic weight through their gate terminals independently [138]. This will endow synaptic circuits with more flexibility in single transmission and learning behavior, hence facilitating

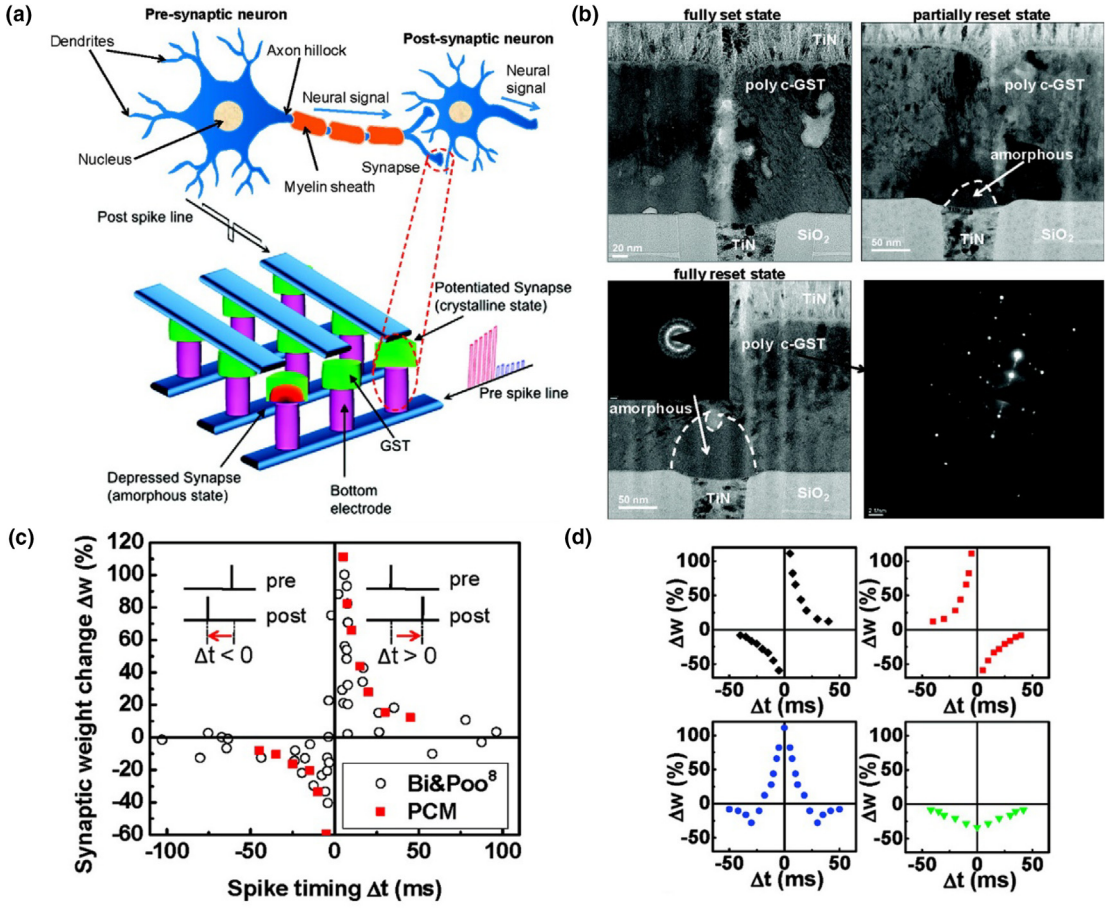

FIGURE 7

(a) Schematic illustration of biological synaptic system and GST-based phase change synaptic memory arrays. The artificial synaptic system is composed of postspike and prespike sandwiching PCM synapses later. (b) TEM images of GST-based synapses in different programmed states (fully set: 500 Ω; partially reset: 0.2 MΩ; fully reset: 2 MΩ;). (c) The measured change of the GST-based synaptic weight versus the relative timing Δt of prespikes and postspikes. For comparison, the STDP characteristics of hippocampal glutamatergic synapses is also presented. (d) Four forms of STDP learning rules, including asymmetric STDP with potentiation (positive Δt, upper left), asymmetric STDP with depression (positive Δt, upper right), symmetric STDP with potentiation ($\Delta t = 0$, lower left), symmetric STDP with depression (all Δt, lower right), were performed. Reproduced with permission [90].

the implementation of more complex synaptic functions. To date, FET-based synapses have been studied by several groups.

In 2013, Chen et al. reported a FET-based synapse that employed a single-walled carbon nanotube (CNT) network as transistor channel [76]. Dynamic interactions between CNT network and hydrogen ions from the poly (ethylene glycol) were attributed to the working mechanism. Synaptic events such as LTP, LTD, and STDP with low powerconsumption were obtained due to the unique electronic characteristic of CNT. Synaptic transistors based on random CNT network channel were also reported by Choi's group in 2017 [116]. The encoding of the synaptic-weight plasticity was achieved by tuning the quantity of carrier injection through embedding Au film as floating gate into the gate dielectric. In addition, pattern recognition in this CNT-based transistor array was demonstrated by employing the most studied case of handwritten number recognition, adopting the MINIST database. In 2016, Wang et al. reported a FET device with anisotropic synaptic characteristics based on a black phosphorus (BP)/phosphorus oxide (PO_x) heterostructure [89]. The authors assumed that the anisotropy of synaptic device was stemmed from the low of crystal symmetry BP channel. Through modulating of the charge transfer between BP channel and PO_x layer, synaptic learning rules including LTP, LTD, and STDP were simulated. Furthermore, an integrated neuromorphic network with anisotropic characteristics was demonstrated by utilizing a high-density BP as channel materials.

In another aspect, nanoparticle organic memory field effect transistor (NOMFET) combining the amplification property of transistors and the charge-trapping effect of memories is considered as a good candidate for emulation of artificial synapses [77,139,140]. Desbief et al. reported artificial synapses based on NOMFET device, in which gold nanoparticle-functionalized SiO_2 was utilized as the dielectric layer [141]. The NOMFET device could be programmed to mimic a depressing or facilitating synapse under a low operation voltage, approximately 1 V. To get in-depth understanding of this synapsetransistor, a series of *in situ* investigation had been implemented, which implied that the transport behavior and morphology of pentacene played vital roles in this low-voltage operation and time-constant artificial synapse.

A large biomolecule (i.e., chitosan) can be utilized either as a gate dielectric layer or a flexible substrate for FET-based synaptic

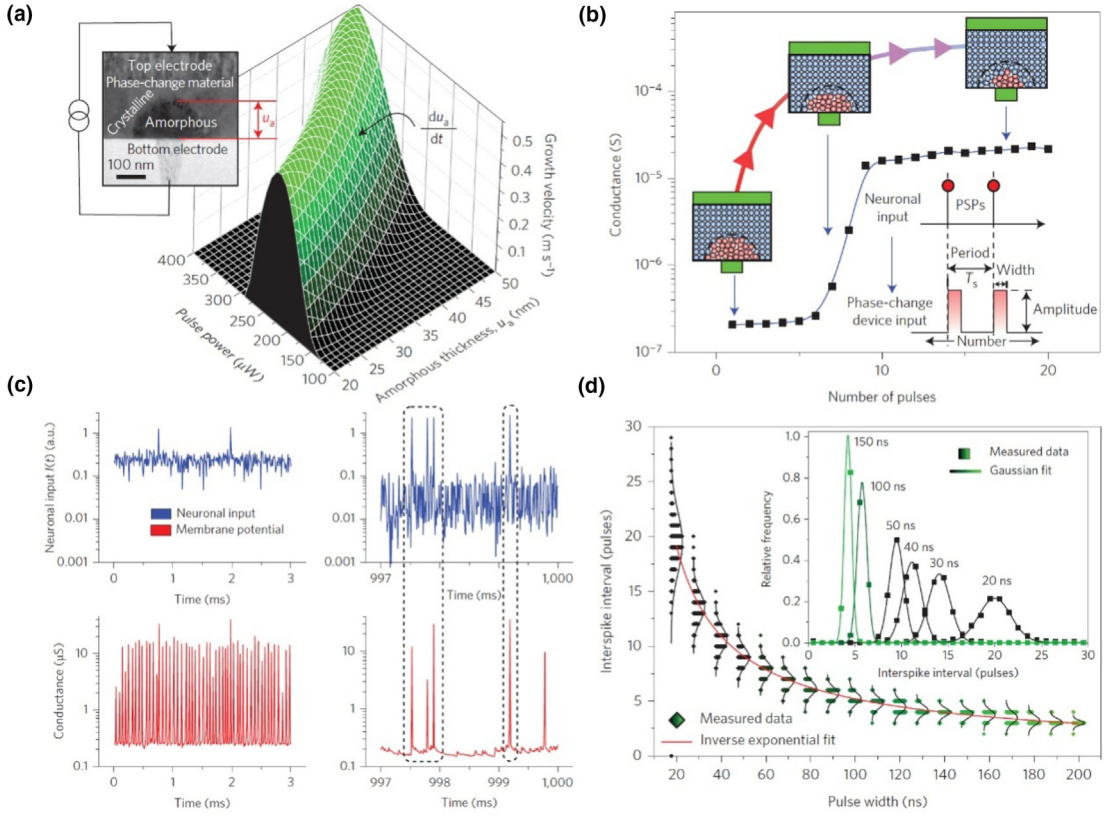

FIGURE 8

(a) Schematic illustration of GST-based phase change neurons, as well as the relationship between the membrane potential and the applied pulse power. (b) The conductance change of the GST-based phase change memory device triggered by the treatment of a train of crystallizing pulses (duration: 50 ns; period: 100 ns). (c) The change of the neuronal input (top) and the obtained membrane potential (bottom), induced by 1000 applied streams of binary events. (d) The interspike intervals is plotted as a function of pulse width in a single neuron. Reproduced with permission [75].

devices as well. In 2014, Wu et al. demonstrated an artificial synapse on paper substrates using chitosan as gate dielectric layer [142]. Implementation of synaptic behaviors, including excitatory postsynaptic current, PPF, dynamic filtering, and spatiotemporally correlated signal processing,was benefited from high proton conductivity (6×10^{-3} S·cm^{-1}) of acetic acid-doped chitosan dielectric. In 2016, Wan et al. demonstrated an artificial synaptic transistor on flexible chitosan membrane [115]. The chitosan membrane simultaneously acted as mechanical support and a gate dielectric for the FET-based synapse. The artificial synapse exhibited quite low energy consumption in each synaptic event (3.9 pJ). In addition, the transformation from short-term memory to long-term memory can be realized in the artificial synapse through repeatedly applying high-amplitude input pulses. Subsequently, in 2016, a biodegradable FET-based synapse employed chitosan film as gate dielectric was reported by the same research group [143]. Synaptic learning rules, including paired-pulse facilitation (PPF) and synaptic filtering, were emulated. In addition, by the treatment of deionized water, the synaptic device could be completely decomposed within 30 min. In 2016, Gou et al. fabricated artificial electric double-layer (EDL) FET-based synapses by employing chitosan and SnO_2 nanowires as gate dielectric and channel, respectively [144]. In response to a positive gate voltage, a strong EDL effect occurred at the chitosan/channel interface that originated from protons migration. In these chitosan-based synapses, protons in the gate dielectric were employed as neurotransmitters to modulate the SnO_2 channel conductance, as well as control the synaptic weight. Similarly, in 2016, Wu et al. demonstrated EDL FET-based synapses based on organic (egg albumen)/inorganic hybrid transistors [145]. The egg albumen dielectric exhibited high ionic conductivity owing to its abundant hydrophilic functional groups, including carboxyl, hydroxy, amidogen, and sulfhydryl. In addition to PPF and dynamic filtering, excitatory postsynaptic current summation and shunting inhibition were mimicked via a transistor system with two in-plane gate structure. Recently, Di et al. reported an artificial chitosan-based tactile-perception system that consisted of a pressure-responsive FET and a signal-processing FET, which was capable of simultaneously transforming and processing signals in a single device (Figure 9) [137]. In this tactile-perception system, the gate voltage and the channel current were employed as the pre-synaptic signal and post-synaptic activity, respectively. By adding a presynaptic spike of −10 V for 50 ms to the gate electrode, the protons move toward the gate electrode, thus induce a postsynaptic current as a result of the accumulation of holes at the chitosan/PDPP3T semiconductor interface. Moreover, the tactile-perception system could simultaneously sense and respond to pressure stimuli and synapse-like processing.

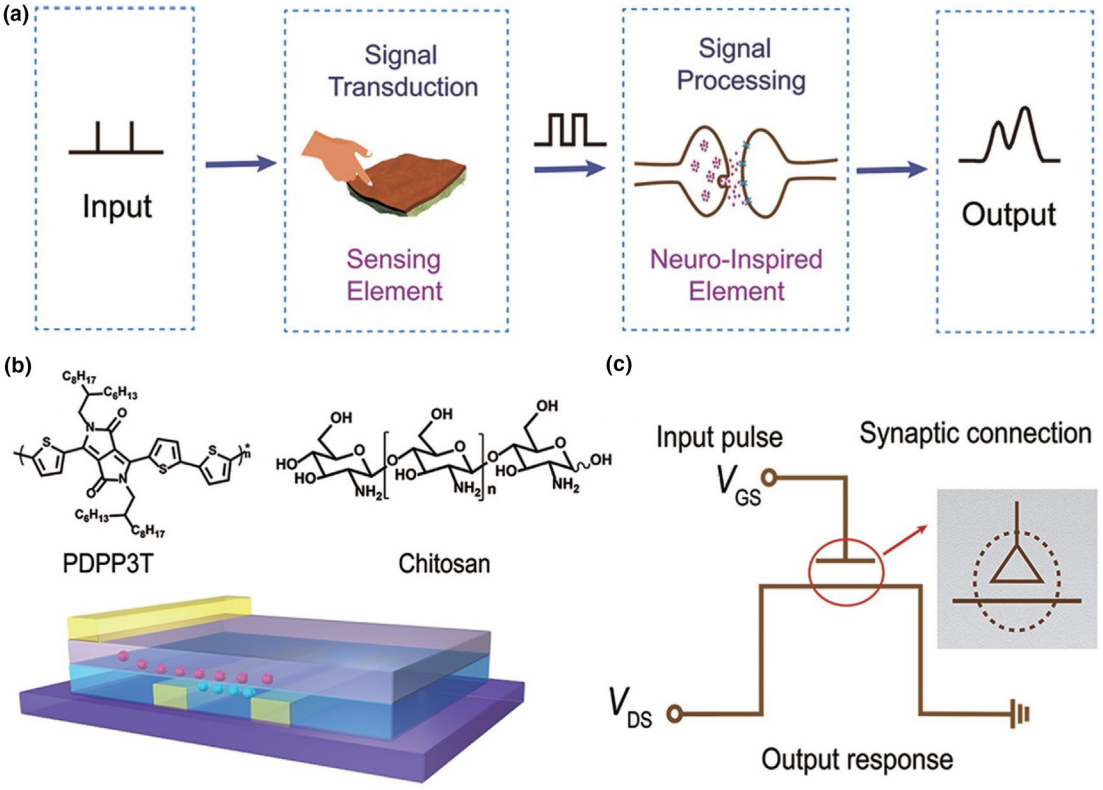

FIGURE 9

(a–c) Schematic illustrations of the process of signal processing of artificial synaptic systems (a), the molecular structures of organic layer (PDPP3T and chitosan) and schematic illustration of the fabricated synaptic transistor (b), and electrical circuit of the artificial synaptic system (c). Reproduced with permission [137].

Conclusions and outlook

Research activities in biomemories have been primarily driven by the search for building blocks of biomolecule-based memories with high biocompatibility and emulation of the artificial synapse. Nevertheless, the challenges remain in the ambiguous mechanism of switching behavior, inferior biocompatibility of hybrid structure, and device variability.

Ambiguous mechanism of switching behavior

Recent progress of biomolecule-base memory devices is summarized in the first section of the review. These devices are fabricated by various kinds of biomolecule units, including protein (silk, ferritin, and myoglobin), saccharide (chitosan and starch), DNA, RNA, and tobacco mosaic virus, and the reversible change between a high resistance state and a low resistance state can be obtained via the application of external electric bias. However, recognizing different switching mechanism of biomolecule-based memory devices, including metal conductive filament formation, space charge and traps, ion conduction, charge transfer, and conformal change, is of great importance. The mechanism of resistive switching effect of these biomolecules is still ambiguous due to the complicated structure of biomolecules. These structures can be easily varied by external stimuli such as temperature, suggesting the complicated formulation of the materials selection criteria. Hence, the exploration of the switching mechanism requires interdisciplinary investigations from viewpoints of structural biology, electronics, and crystallography. For example, *in situ* HRTEM, XPS, UPS, CAFM, and Kelvin probe microscope can be used to study the physical behavior and dynamic properties of diffusive memory devices. Besides, density function theory (DFT) calculations can also be used to reveal the microscopic mechanism by simulating the optimized structures and electronic properties of the active layer.

Inferior biocompatibility of a hybrid structure

Typical metal-insulator-metal (MIM) structure with a hybrid active layer is employed for most of the biomolecule-based memories, and some of them use biomolecule–nanoparticle composite as the active layer. Thus, negative effect on the biocompatibility of the entire devices can be inevitably brought by the introduction of requisite non-degradable organic or inorganic building blocks' components into the hybrid switching layer, which hinders the development of implantable and biocompatible memory devices. Particularly, interactions between artificial electronic devices and living systems usually initiate at the electronics/biology interfaces. Therefore, it is of great importance to develop biocompatible materials and use them as coated interfacial layer of electronic devices to promote biocompatibility. Additionally, flexibility and softness are also desirable characteristics to increase the biocompatibility of electronic devices with the surrounding biological tissues and organs.

Device variability

The variance from device to device, as well as switching cycle to cycle, sometimes must not be disregarded. Delicate selection of biomaterials based on the in-depth understanding of their biological, chemical, physical, and electrical properties can induce a stable system and significantly reduce variance from cycles, while the variances from device to device mainly derived from the random filament-forming process with a different structure in each cell. Engineering of film morphology to reduce random fabrication of active layer is crucial to avoid such variety. Scaling down the size of devices to which is comparable to the filament size, and thus producing a limited active area has been suggested a way to resolve this problem.

The ability to scale down and fabricate high-density biomolecule-based data storages could certainly promote relevant real device applications. There are mainly two strategies to realize this objective. The first strategy is to utilize traditional semiconductor fabrication processes to scale down biomolecule-based devices such as lithography, deposition, and etching which are compatible with CMOS techniques [43]. However, being the intrinsic limitation, Moore's law is expected to reach its bottleneck by 2022 owing to technical complexity, according to the latest 'International Technology Roadmap for Semiconductors'. The second strategy is exploring multilevel data storage in a single device that could realize high-density data storage based on biopolymers such as lignin and sericin. [41,113]. Although the above-mentioned challenges remain to be addressed, we believe that biomolecule-based memory devices will facilitate the development of a variety of electronic and biological practical applications. For example, the imperceptible state of biomaterials is indispensable for building a seamless bridge to connect our soft human organ and tissue with electronic devices. Using biomolecules to prepare lightweight memory systems can well meet this criterion. Ultra-lightweight memory systems (normally less than 1 $mg{\cdot}cm^{-2}$) have been manufactured based on silk fibroin, which will endow electronic devices with imperceptible feature and excellent biocompatibility, thus promoting the applications in the development of smart electronic skins, implantable chips, health monitors, and wearable devices.

Unsatisfied realization of performance gains

In the second part, recent progress of artificial synaptic memory and integrated neuromorphic categorized into memristor, phase change memory, and FET device have been summarized. Through these synaptic memories and systems, figure of merits of synaptic and neural functions (plasticity and elasticity) such as STDP, STP, LTP, STD, paired-pulse facilitation, and self-learning ability have been mimicked. Nevertheless, operation with the targeted energy efficiency, while no impact on accuracy, is a big challenge since the major impediment still exists at the cell level. For example, state-of-art memristors suffer from write nonlinearities and excessive write noise, as well as high write biases. Lowering the noise and switching voltage in the two terminal devices without compromising on data retention capability has been proven difficult. In another aspect, these limitations reduce the scalability of filament-forming material-based memristors and phase change memories, as well as hinder these devices to approach the high efficiency of the human brain. Memristors based on organic materials, which are benefited from added functionality, low-power consumption, and low-cost manufacturing, may open a tantalizing way to construct advanced neural prostheses. In another aspect, conquering the inherent limitations of organic materials such as slow kinetics of ion diffusion in organic materials to maintain the states should be investigated.

Synaptic elasticity and plasticity functions contribute to memory and learning ability of biological synapse. Fabricating electric memory devices that exhibit most of these synaptic functions and realize and parallel process a series of information simultaneously might be necessary. The fusion of biological knowledge and electronic science in the design of artificial synapse will enable efficient emulation of various synaptic functions, as well as more sophisticated functionalities, of biological neural networks.

Although a series of existing basic and technical challenges that need to be overcome, based on these aforementioned artificial synapses and neuromorphic networks, we believe that artificial brain and smart electronic device will be fabricated in the future. Benefiting from this imagine, health solution will be provided for patients with brain diseases such as Alzheimer's and Parkinson's disease by transplantation of an artificial brain. Up to now, papers regarding biomaterial-based artificial synapses are rarely reported, whereasa growing number of biomolecule-based artificial synapses are expected to be developed and applied in the coming future. Moreover, numerous electronic devices with artificial intelligence will be developed and bring great development to computer science.

Acknowledgments

The authors acknowledge the grants from RGC of Hong Kong under Grant Nos. C7045-14E and T42-103/16, the Natural Science Foundation of China (Grant Nos. 61601305 and 61604097), the Science and Technology Innovation Commission of Shenzhen (Grant Nos. JCYJ20170302145229928, JCYJ20170302151653768 and KQJSCX20170327150812967), Guangdong Provincial Department of Science and Technology (Grant No. 2017A010103026), the Department of Education of Guangdong Province (Grant Nos. 2015KQNCX141 and 2016KTSCX120), the Natural Science Foundation of SZU (STH) and City University of Hong Kong project number 7004378.

References

[1] Q.D. Ling et al., Prog. Polym. Sci. 33 (2008) 917–978.
[2] S.T. Han, Y. Zhou, V.A. Roy, Adv. Mater. 25 (2013) 5425–5449.
[3] T.W. Kim et al., NPG Asia Mater. 4 (2012) 12.
[4] H.J. Yen et al., Polymers 9 (2017) 25.
[5] C.W. Chu et al., Adv. Mater. 17 (2005) 1440–1443.
[6] M.J. Rozenberg, I.H. Inoue, M.J. Sanchez, Appl. Phys. Lett. 88 (2006) 033510.
[7] J.S. Lee et al., Nat. Nanotechnol. 2 (2007) 790–795.
[8] Y. Yang et al., Adv. Funct. Mater. 16 (2006) 1001–1014.
[9] O. Kahn, C.J. Martinez, Science 279 (1998) 44–48.
[10] K. Roy et al., Nat. Nanotechnol. 8 (2013) 826–830.
[11] S.J. Kim, J.S. Lee, Nano Lett. 10 (2010) 2884–2890.
[12] J. Yao et al., Nat. Commun. 3 (2012) 1101.
[13] S.-T. Han et al., Small 12 (2016) 390–396.
[14] Y. Yan et al., RSC Adv. 5 (2015) 64471–64477.
[15] S.-T. Han et al., J. Mater. Chem. C 3 (2015) 3173–3180.
[16] J.B. Cui et al., Appl. Phys. Lett. 81 (2002) 3260–3262.

[17] M.C. Tsai et al., Polym. Chem. 7 (2016) 2780–2784.
[18] News, http://www.icinsights.com/news/bulletins/Total-Memory-Market-Forecast-To-Increase-10-In-2017/, August, 2017.
[19] M. Irimia-Vladu et al., Mater. Today 15 (2012) 340–346.
[20] M.J. Tan et al., J. Mater. Chem. C 4 (2016) 5531–5558.
[21] Y. Li et al., J. Environ. Monit. 10 (2008) 1233–1238.
[22] K. Breivik et al., Environ. Sci. Technol. 48 (2014) 8735–8743.
[23] M. Irimia-Vladu, Chem. Soc. Rev. 43 (2014) 588–610.
[24] B. Zhu et al., Adv. Mater. 28 (2016) 4250–4265.
[25] M. Irimia-Vladu et al., Adv. Funct. Mater. 20 (2010) 4069–4076.
[26] M. Irimia-Vladu, N.S. Sariciftci, S. Bauer, J. Mater. Chem. 21 (2011) 1350–1361.
[27] S.W. Hwang et al., Adv. Mater. 26 (2014) 1992–2000.
[28] S.J. Kim et al., ACS Appl. Mater. Interfaces 7 (2015) 4869–4874.
[29] R.R. Birge et al., J. Phys. Chem. B 103 (1999) 10746–10766.
[30] D.H. Kim et al., Science 333 (2011) 838–843.
[31] A. Chortos, J. Liu, Z.N. Bao, Nat. Mater. 15 (2016) 937–950.
[32] B.C.K. Tee et al., Science 350 (2015) 313–316.
[33] D. Son et al., Nat. Nanotechnol. 9 (2014) 397–404.
[34] D. Kuzum, S.M. Yu, H.S.P. Wong, Nanotechnology 24 (2013) 382001.
[35] D.S. Jeong et al., RSC Adv. 3 (2013) 3169–3183.
[36] S.W. Hwang et al., Science 337 (2012) 1640–1644.
[37] Z.H. Chen et al., J. Mater. Chem. B 5 (2017) 3163–3171.
[38] P. Lin, F. Yan, Adv. Mater. 24 (2012) 34–51.
[39] L. Torsi et al., Chem. Soc. Rev. 42 (2013) 8612–8628.
[40] N. Raeis-Hosseini, J.S. Lee, J. Electroceram. (2017), https://doi.org/10.1007/s10832-017-0104-z.
[41] H. Wang et al., Adv. Mater. 25 (2013) 5498–5503.
[42] Y. Ko, S.W. Ryu, J. Cho, Appl. Surf. Sci. 368 (2016) 36–43.
[43] F.B. Meng et al., Small 10 (2014) 277–283.
[44] N. Gogurla et al., Nanotechnology 24 (2013) 345202.
[45] F. Meng et al., Small 7 (2011) 3016–3020.
[46] Y.C. Chang, Y.H. Wang, A.C.S. Appl, Mater. Interfaces 6 (2014) 5413–5421.
[47] J.W. Chang et al., Adv. Mater. 23 (2011) 4077–4081.
[48] Y.C. Chen et al., Sci. Rep. 5 (2015) 10022.
[49] S.C. Qin et al., Org. Electron. 22 (2015) 147–153.
[50] K. Qian et al., J. Mater. Chem. C 4 (2016) 9637–9645.
[51] J. Credou, T. Berthelot, J. Mat. Chem. B 2 (2014) 4767–4788.
[52] Z.X. Lim, K.Y. Cheong, Phys. Chem. Chem. Phys. 17 (2015) 26833–26853.
[53] G.H. Altman et al., Biomaterials 24 (2003) 401–416.
[54] H. Tao, D.L. Kaplan, F.G. Omenetto, Adv. Mater. 24 (2012) 2824–2837.
[55] Y. Cao, B.C. Wang, Int. J. Mol. Sci. 10 (2009) 1514–1524.
[56] C.Y. Jiang et al., Adv. Funct. Mater. 17 (2007) 2229–2237.
[57] C.H. Wang, C.Y. Hsieh, J.C. Hwang, Adv. Mater. 23 (2011) 1630–1634.
[58] S. Diano et al., Nat. Neurosci. 9 (2006) 381–388.
[59] M. Tsodyks, K. Pawelzik, H. Markram, Neural Comput. 10 (1998) 821–835.
[60] D.L. Schacter, Searching for Memory: The Brain, the Mind, and the Past, Basic Books, 2008.
[61] P.A. Merolla et al., Science 345 (2014) 668–673.
[62] T. Ohno et al., Nat. Mater. 10 (2011) 591–595.
[63] J. Tonnesen et al., Nat. Neurosci. 17 (2014) 678–685.
[64] A.E. Pereda, Nat. Rev. Neurosci. 15 (2014) 250–263.
[65] J. Dubnau, A.S. Chiang, T. Tully, J. Neurobiol. 54 (2003) 238–253.
[66] E.R. Kandel, Science 294 (2001) 1030–1038.
[67] S.M. Yu et al., IEEE Trans. Electron Devices 58 (2011) 2729–2737.
[68] C.C. Zhang et al., J. Mater. Chem. C 4 (2016) 3217–3223.
[69] Y. Nishitani et al., Jpn. J. Appl. Phys. 52 (2013). 04CE06.
[70] M.K. Benna, S. Fusi, Nat. Neurosci. 19 (2016) 1697–1706.
[71] S. Mandal et al., Sci. Rep. 4 (2014) 5333.
[72] C. Du et al., Adv. Funct. Mater. 25 (2015) 4290–4299.
[73] S.H. Jo et al., Nano Lett. 10 (2010) 1297–1301.
[74] Z. Wang et al., Nat. Mater. 16 (2017) 101–108.
[75] T. Tuma et al., Nat. Nanotechnol. 11 (2016) 693–699.
[76] K. Kim et al., Adv. Mater. 25 (2013) 1693–1698.
[77] F. Alibart et al., Adv. Funct. Mater. 20 (2010) 330–337.
[78] F. Alibart et al., Nanotechnology 23 (2012) 075201.
[79] A. Serb et al., Nat. Commun. 7 (2016) 12611.
[80] M. Prezioso et al., Nature 521 (2015) 61–64.
[81] G. Indiveri et al., Front. Neurosci. 5 (2011) 73.
[82] G. Indiveri et al., Nanotechnology 24 (2013) 384010.
[83] C.S. Poon, K. Zhou, Front. Neurosci. 5 (2011) 108.
[84] M.J. Wall, M.M. Usowicz, Nat. Neurosci. 1 (1998) 675–682.
[85] J.J. Yang, D.B. Strukov, D.R. Stewart, Nat. Nanotechnol. 8 (2013) 13–24.
[86] H. Wang et al., Small 12 (2016) 2715–2719.
[87] N.R. Hosseini, J.S. Lee, ACS Nano 9 (2015) 419–426.
[88] B. Sun et al., J. Mater. Chem. C 3 (2015) 12149–12155.
[89] H. Tian et al., Adv. Mater. 28 (2016) 4991–4997.
[90] D. Kuzum et al., Nano Lett. 12 (2012) 2179–2186.
[91] A. Garg, J.N. Onuchic, V. Ambegaokar, J. Chem. Phys. 83 (1985) 4491–4503.
[92] J.H. Lee et al., Chem. Commun. 48 (2012) (2010) 12008–12010.
[93] C. Zhang et al., Chem. Commun. 52 (2016) 4828–4831.
[94] B.J. Kim et al., Small 9 (2013) 3784–3791.
[95] N.R. Hosseini, J.S. Lee, Adv. Funct. Mater. 25 (2015) 5586–5592.
[96] N. Raeis-Hosseini, J.S. Lee, A.C.S. Appl, Mater. Interfaces 8 (2016) 7326–7332.
[97] S.O. Kelley, J.K. Barton, Science 283 (1999) 375–381.
[98] R.P. Goodman et al., Nat. Nanotechnol. 3 (2008) 93–96.
[99] R. de la Rica, H. Matsui, Chem. Soc. Rev. 39 (2010) 3499–3509.
[100] J.C.M. van Hest, D.A. Tirrell, Chem. Commun. (2001) 1897–1904.
[101] Z.Y. Lv et al., ACS Appl. Mater. Interfaces 7 (2015) 27223–27233.
[102] I. Medalsy et al., Nat. Nanotechnol. 5 (2010) 451–457.
[103] Y. Ko et al., ACS Nano 5 (2011) 9918–9926.
[104] M.K. Hota et al., Adv. Funct. Mater. 22 (2012) 4493–4499.
[105] H. Wang et al., Adv. Funct. Mater. 25 (2015) 3825–3831.
[106] H. Wang et al., Small 12 (2016) 3360–3365.
[107] Y.C. Chiu et al., Adv. Mater. 27 (2015) 6257–6264.
[108] P.X. Guo, Nat. Nanotechnol. 5 (2010) 833–842.
[109] T. Lee et al., ACS Nano 9 (2015) 6675–6682.
[110] P. Stadler et al., Org. Electron. 8 (2007) 648–654.
[111] R.J. Tseng et al., Nat. Nanotechnol. 1 (2006) 72–77.
[112] G. Zhou et al., Curr. Appl. Phys. 17 (2017) 235–239.
[113] Y. Park, J.S. Lee, A.C.S. Appl, Mater. Interfaces 9 (2017) 6207–6212.
[114] Y. van de Burgt et al., Nat. Mater. 16 (2017) 414–418.
[115] Y.H. Liu et al., Adv. Mater. 27 (2015) 5599–5604.
[116] S. Kim et al., ACS Nano 11 (2017) 2814–2822.
[117] L.Q. Zhu et al., Nat. Commun. 5 (2014) 3158.
[118] L.Q. Zhu et al., ACS Appl. Mater. Interfaces 8 (2016) 21770–21775.
[119] S.J. Martin, P.D. Grimwood, R.G.M. Morris, Annu. Rev. Neurosci. 23 (2000) 649–711.
[120] T.V.P. Bliss, G.L. Collingridge, Nature 361 (1993) 31–39.
[121] D.M. Bannerman et al., Nat. Rev. Neurosci. 15 (2014) 181–192.
[122] Q.F. Xia et al., Nano Lett. 9 (2009) 3640–3645.
[123] Y. Park, J.S. Lee, ACS Nano 11 (2017) 8962–8969.
[124] S. Kim et al., ACS Nano 8 (2014) 10262–10269.
[125] S. Kim, S. Choi, W. Lu, ACS Nano 8 (2014) 2369–2376.
[126] S. Kim et al., Nano Lett. 15 (2015) 2203–2211.
[127] A. Nayak et al., Adv. Funct. Mater. 22 (2012) 3606–3613.
[128] G. Palma, et al., IEEE/ACM International Symposium on Nanoscale Architectures (NANOARCH) (2013) 95–100.
[129] C. Yoon et al., Nano Lett. 17 (2017) 1949–1955.
[130] S.G. Hu et al., Nat. Commun. 6 (2015) 7522.
[131] S. Raoux, W. Welnic, D. Ielmini, Chem. Rev. 110 (2010) 240–267.
[132] S.B. Eryilmaz et al., IEEE Trans. Electron Devices 63 (2016) 5004–5011.
[133] K. Nakayama et al., Jpn. J. Appl. Phys. Part I (39) (2000) 6157–6161.
[134] Y. Li et al., Sci. Rep. 3 (2013) 1619.
[135] S. Kim, et al., IEEE Symposium on VLSI Technology (2012) 155–156.
[136] M.D. Pickett, G. Medeiros-Ribeiro, R.S. Williams, Nat. Mater. 12 (2013) 114–117.
[137] Y. Zang et al., Adv. Mater. 29 (2017) 1606088.
[138] P. Balakrishna Pillai, M.M. De Souza, ACS Appl. Mater. Interfaces 9 (2017) 1609–1618.
[139] S.-T. Han et al., Nanoscale 7 (2015) 17496–17503.
[140] Y. Zhou et al., Nanotechnology 24 (2013) 205202.
[141] S. Desbief et al., Org. Electron. 21 (2015) 47–53.
[142] G. Wu et al., J. Mater. Chem. C 2 (2014) 6249–6255.
[143] R. Liu et al., J. Mater. Chem. C 4 (2016) 7744–7750.
[144] G. Gou et al., J. Mater. Chem. C 4 (2016) 11110–11117.
[145] G. Wu et al., Sci. Rep. 6 (2016) 23578.